

# Development of a Robust Anti-Islanding Algorithm for Utility Interconnection of Distributed Fuel Cell Powered Generation

Chuttchaval Jeraputra and Prasad N. Enjeti, *Fellow, IEEE*

**Abstract**—In this paper, a robust anti-islanding algorithm for distributed fuel cell powered generation (DFPG) is proposed. Three different islanding scenarios are explored and presented based on analysis of real and reactive power mismatch. It is shown via analysis that islanding voltage is a function of real power alone, whereas its frequency is a function of both real and reactive power. Following this analysis, a robust anti-islanding algorithm is developed. The proposed algorithm continuously perturbs ( $\pm 5\%$ ) the reactive power supplied by DFPG while simultaneously monitoring the utility voltage and frequency. If islanding were to occur, a measurable frequency deviation takes place upon which the real power of DFPG is further reduced to 80%; now a drop in voltage positively confirms islanding, and the DFPG is safely disconnected. This method of control is shown to be robust, able to detect islanding under resonant loads, and fast acting (operable in one cycle). Possible islanding conditions are simulated and verified with analysis. Experimental results on a 0.5-kW fuel cell inverter system connected to 120-V 60-Hz utility are discussed.

**Index Terms**—Anti-islanding algorithm, distributed fuel cell powered generation (DFPG), islanding.

## I. INTRODUCTION

LOW COST and clean performance benefits have influenced fuel cell as a preferred choice for utility interactive distributed power generation. Fig. 1 shows the typical distributed fuel cell powered generation (DFPG) connected to utility [1]. However, interconnection of DFPG with utility raises several major issues and technical difficulties. Islanding is an important issue of concern as more and more independently controlled DFPG systems are connected to the power distribution system. Islanding phenomenon occurs when utility is intentionally or accidentally disconnected from network and the DFPG continues to energize local loads. This condition causes danger to maintenance personnel arriving to service energized isolated feeder [2]. Further, unsynchronized reclosure of utility to formed isolated loads results in damages to fuel cell inverters. This concern is addressed in IEEE Std. 929-2000 [3] and IEEE Std. 1547 [4].

Several islanding detection algorithms have been developed in the past decade [5]–[10]. These algorithms can be categorized into two major approaches.

Manuscript received August 19, 2003; revised June 3, 2004. Recommended by Associate Editor M. Ropp.

The authors are with the Power Electronics and Power Quality Laboratory, Electrical Engineering Department, Texas A&M University, College Station, TX 77843-3128 USA (e-mail: enjeti@ee.tamu.edu; p.enjeti@ieee.org; cxj20@ee.tamu.edu).

Digital Object Identifier 10.1109/TPEL.2004.833439

### Passive

- Over/under voltage and frequency detection [5].
- Phase jump detection [5].
- Voltage harmonic monitoring [6].

### Active

- Output power variation [7].
- Active frequency drift [8], [9].
- Sliding mode frequency shift [8], [10].

Over/under voltage and frequency detection approach, the inverter is shut down when the utility voltage/frequency deviates from set values. While the method is simple, it fails to detect islanding when the inverter generated power closely matches with the connected loads [11]. In the phase jump detection method, the phase of inverter current is instantaneously synchronized at zero crossing with phase of voltage via phase lock loop (PLL) circuitry. Considerable phase difference can be identified as an occurrence of islanding. However, this method fails when the load power factor is unity [11]. In the voltage harmonic monitoring method, it is envisioned that in the absence of the utility (islanding) results in excessive harmonic voltage due to magnetizing current drawn by power transformers etc., [2], [11]. However, setting an appropriate harmonic threshold to disconnect the inverter is nearly impossible due to presence of non-linear loads. This renders the harmonic monitoring method as impractical [6].

Active methods try to overcome the shortcomings of passive methods by introducing perturbations in the inverter output. In the output power variation method, the inverter real power is periodically perturbed, and the voltage is continuously monitored. When islanding occurs, voltage fluctuations become apparent due to real power mismatch. This information is used to initiate shut down procedure. This method requires multiple DFPGs connected to the utility to be synchronized. If synchronization is not done, the method becomes ineffective due to the averaging effect [7]. Active frequency drift (AFD) method introduces small increase/decrease in the frequency of inverter output current while monitoring the frequency of the voltage. A measurable deviation in frequency of the voltage indicates islanding. However, this method has been shown to fail when the load phase angle matches with the phase offset generated by perturbing the frequency [8], [12]. Sliding mode frequency shift (SMS) method applies similar strategy as AFD. In this method, the starting angle of inverter current is controlled. Under islanding, a measurable frequency deviation is observed. This method also fails when the load phase angle equals the starting angle [8], [12], [13].

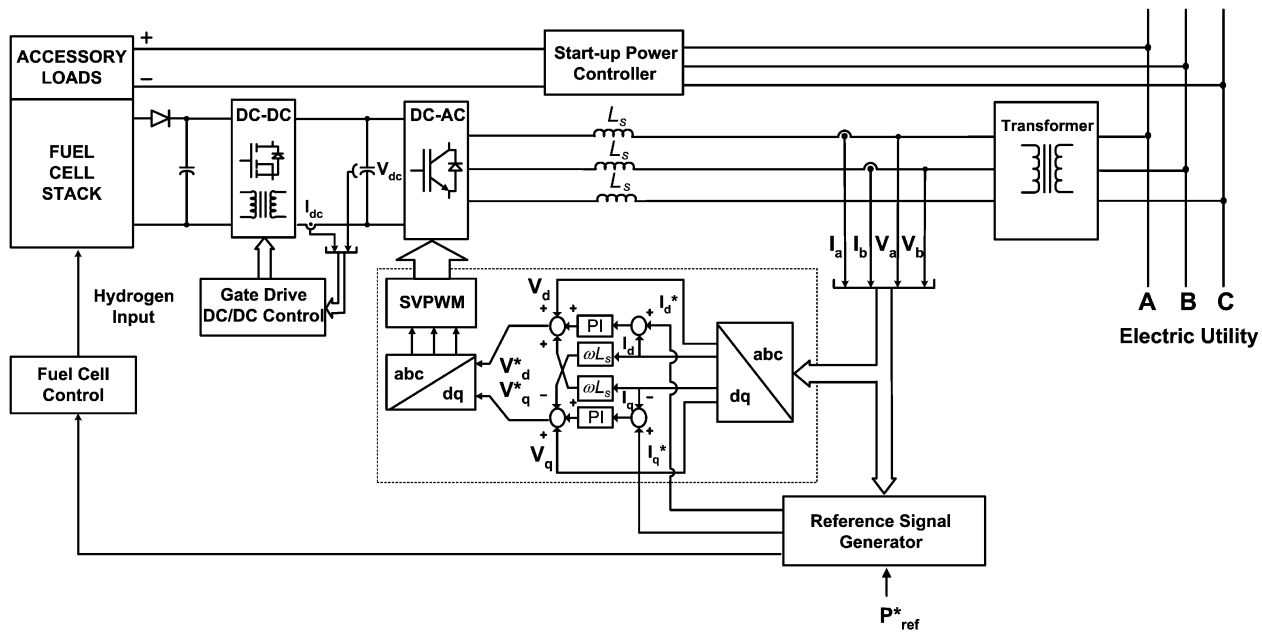


Fig. 1. Fuel cell power conditioner control system for supplying power to the utility (utility interface).

In response to these concerns, this paper explores the development of a robust anti-islanding algorithm. The proposed algorithm continuously perturbs ( $\pm 5\%$ ) the reactive power supplied by DFPG while monitoring the utility voltage and frequency. It is shown that by perturbing DFPG reactive power by  $\pm 5\%$  results in observable frequency deviation ( $> \pm 1\%$ ) when islanding occurs. To further positively confirm islanding, the proposed algorithm reduces the DFPG real power output to 80%. If the terminal voltage drops below 0.9 per-unit, the DFPG is disconnected. This method of detection is shown to be robust and fast acting (operable in one cycle) and it significantly reduces the nondetection zone (NDZ) compared to all other detection method. Several possible islanding conditions are simulated and verified with analysis. Experimental results, on a 0.5-kW fuel cell inverter connected to 120-V 60-Hz utility are discussed.

## II. ANALYSIS OF REAL AND REACTIVE POWER MISMATCH

Islanding voltage and frequency can be calculated analytically based on real and reactive power mismatch at the instant the utility disconnected. Fig. 2(a) shows power flow diagram of DFPG and connected load in the presence of utility. Fig. 2(b) shows the utility disconnected and  $\Delta P$  and  $\Delta Q$  are defined as real and reactive power mismatches at the instant of disconnection.

For the purpose of analysis, DFPG is modeled as a current source and the load is represented by equivalent parallel RLC elements. Per phase equivalent circuit of the system for this condition is shown in Fig. 3.

For clarity, the term “islanding voltage  $V_i$ ” is defined as the voltage at inverter terminal and the load terminals. The term “islanding frequency  $\omega_i$ ” is defined as the frequency of inverter output when the utility is disconnected.

Let

$P_I$  real power output of the DFPG;  
 $Q_I$  reactive power output of DFPG;  
 $P_G$  real power output of the utility;

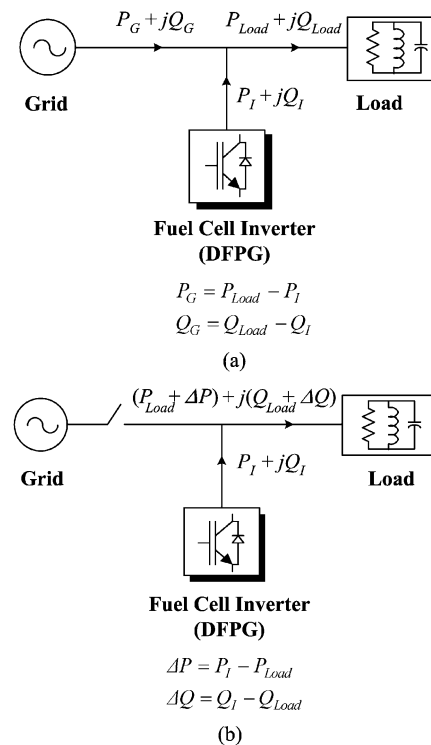


Fig. 2. Interconnection of DFPG source to the utility and the load: (a) normal condition and (b) under islanding showing the power mismatch at the instant the utility is disconnected.

$Q_G$  reactive power output of the utility;  
 $Q_C$  capacitive reactive power (of the load);  
 $Q_L$  inductive reactive power (of the load);  
 $\Delta P$  real power mismatch between DFPG and utility;  
 $\Delta Q$  reactive power mismatch between DFPG and utility;  
 $V_i$  islanding voltage;  
 $V_n$  nominal system voltage.

Since the load is represented by equivalent RLC elements which connected in parallel, islanding voltage across R and par-

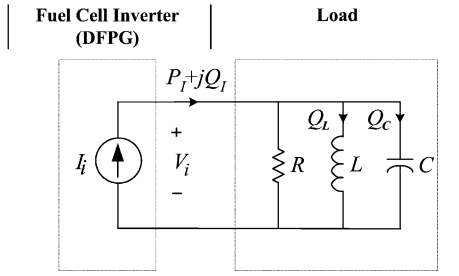


Fig. 3. Equivalent circuit of the DFIG and the load at the instant the utility is disconnected.

allel LC is the same. Impedance of parallel LC (Fig. 3) in a function of frequency is expressed as

$$\text{Im}\{Z_{LC}\} = \frac{\omega_i L}{1 - \omega_i^2 LC} \quad (1)$$

where  $\omega_i$  is the islanding frequency. Further,  $Z_{LC}^*$  can be expressed in terms of  $P_I$  and  $Q_I$  variables as

$$\text{Im}\{Z_{LC}^*\} = \frac{R \cdot P_I}{Q_I}. \quad (2)$$

Equating (1) and (2), we obtain

$$\omega_i^2 - \frac{Q_I}{RC P_I} \omega_i - \left(\frac{1}{\sqrt{LC}}\right)^2 = 0. \quad (3)$$

The quality factor  $q$  of the connected load is defined as [1]

$$q = \frac{\sqrt{|Q_L| \cdot |Q_C|}}{P} = R \sqrt{\frac{C}{L}}. \quad (4)$$

Equation (3) can be expressed in terms of  $q$  as

$$\omega_i^2 - \frac{R}{q^2 L} \frac{Q_I}{P_I} \omega_i - \left(\frac{R}{qL}\right)^2 = 0. \quad (5)$$

From (5), the islanding frequency  $\omega_i$  is expressed as

$$\omega_i \approx \frac{1}{\sqrt{LC}} \cdot \left(\frac{1}{2} \frac{Q_I}{P_I} + 1\right). \quad (6)$$

Voltage at the instant utility disconnected (islanding voltage) can be calculated from

$$\frac{V_I}{V} = \sqrt{\frac{P_I}{P_{\text{Load}}}}. \quad (7)$$

The islanding voltage  $V_i$  can be expressed as

$$V_i = \sqrt{k} \cdot V \quad (8)$$

where

$$k = \frac{P_I}{P_{\text{Load}}}. \quad (9)$$

From the previous analysis the following can be concluded.

- 1) The islanding frequency  $\omega_i$  is a function of DFIG real power ( $P_I$ ), reactive power ( $Q_I$ ), and the resonant frequency of the load ( $1/\sqrt{LC}$ ) as shown in (6).
- 2) Voltage at the inverter terminals at the instant the utility disconnected is a function of the ratio of real power of the DFIG and the load as shown in (8).

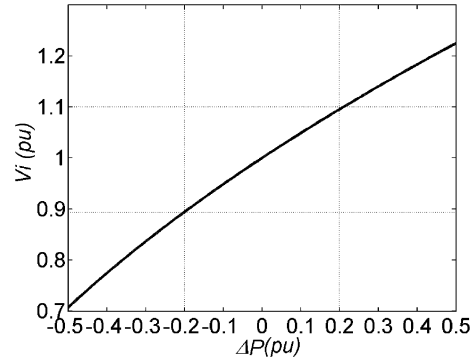


Fig. 4. Variation of islanding voltage  $V_i$  (in Fig. 3) versus  $\Delta P$ .

- 3) Islanding voltage  $V_i$  increases when  $P_I > P_L$  and decreases for vice versa.
- 4) The worst case condition occurs in the following scenario when DFIG real power is equal to the real power of the load, i.e.,  $P_I = P_{\text{Load}}$ , and the corresponding reactive powers are also equal  $Q_I = Q_{\text{Load}}$ . For this condition, the voltage and the frequency at the inverter terminals continues to be the same as when the utility was connected. Under this condition the inverter fails to notice the disconnection of the utility and continues to operate, hence causing islanding. When the above described conditions are nearly met, the variation in voltage and frequency may be small and may escape detection. This zone is called non-detect zone (NDZ).

### III. ROBUST ANTI-ISLANDING ALGORITHM DEVELOPMENT

To detect islanding effectively, it is necessary to have good understanding of all possible islanding conditions. Three major islanding scenarios are explored, and a robust anti-islanding algorithm is developed and presented in this section.

Case 1)  $\Delta P$  is large:

When the real power of DFIG and that of the load are not equal,  $\Delta P$  is large. Under this condition, if the utility is disconnected, then from (8), it is clear that the inverter terminal voltage will vary widely. Fig. 4 shows the variation of the islanding voltage  $V_i$  as a function of  $\Delta P$ . According to the IEEE Std. 929-2000 [3], the inverter operating voltage should be within the range of  $0.88 \leq V_i \leq 1.10$  pu. If these operating limits are chosen, islanding condition can be detected effectively only if  $\Delta P > \pm 20\%$  (Fig. 4).

Case 2)  $\Delta P$  is small and  $\Delta Q$  is large:

In the case the real power of DFIG and the load are nearly equal, i.e.,  $\Delta P$  is small; however, the reactive power of DFIG and the load differ ( $\Delta Q$  difference is larger). Upon disconnection of the utility, the relationship derived in (6) confirms that a change in frequency occurs. Fig. 5(a) shows variation of the islanding frequency as a function of  $\Delta P$  and  $\Delta Q$ . Fig. 5(b) shows islanding frequency variation as a function of  $\Delta Q$  when  $\Delta P$  is zero. It is noted that the variation is also a function of the quality factor  $q$  of load [see (6)]. According to the IEEE

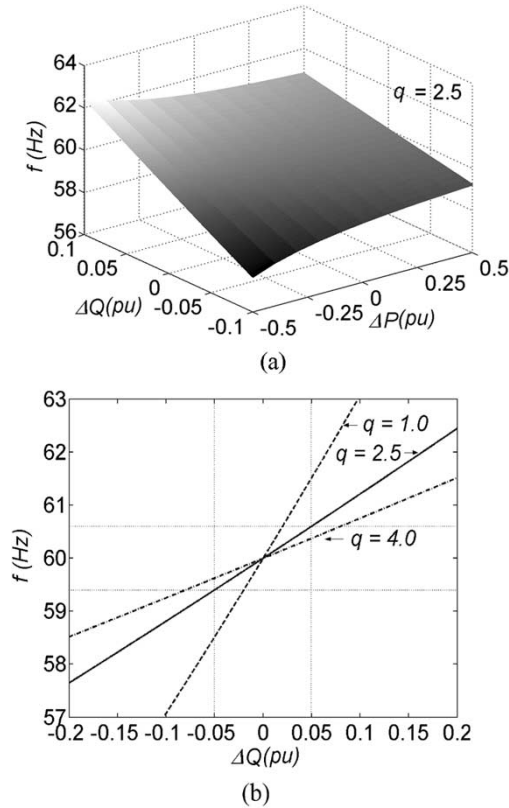


Fig. 5. Variation of islanding frequency: (a) variation of Islanding frequency (in Fig. 2) as a function of  $\Delta P$  and  $\Delta Q$  variables for  $q = 2.5$  and (b) frequency versus  $\Delta Q$  as a function of  $q$  when  $\Delta P \approx 0$ .

Std. 929-2000 [3], the inverter operating frequency should be within the range of 59.3 to 60.5 Hz. Therefore, the DFIG must disconnect when the frequency is out of these limits. However, if this condition is chosen for islanding protection, the inverter (DFPG) will fail to disconnect when the load  $q = 2.5$ ,  $\Delta P = 0$ , and  $\Delta Q < \pm 5\%$  [see Fig. 5(b)].

#### Case 3) $\Delta P$ and $\Delta Q$ are small

It is clear from case 1 and case 2 analysis that a small  $\Delta P$  ( $< \pm 20\%$ ) results in an insufficient change in voltage  $V_i$  (Fig. 4) and small  $\Delta Q$  ( $< \pm 5\%$ ) results in inadequate change in frequency (Fig. 5) to effectively disconnect the DFIG and prevent islanding. This zone is commonly known as nondetection zone (NDZ) for the passive methods to detect islanding and shown in Fig. 6. Thus, the focus of the proposed algorithm in this paper is to reduce the NDZ as detailed in Section IV.

#### IV. PROPOSED POWER CONTROL ALGORITHM

The focus of the proposed algorithm is to reduce the NDZ to near zero. The algorithm consists of two steps. In step 1, the reactive power ( $Q_I$ ) of DFIG is continuously perturbed by  $\pm 5\%$  while maintaining the real power ( $P_I$ ) constant. Both the voltage and frequency simultaneously are monitored. The ratio of  $Q_I$  to  $P_I$  is expressed as

$$\frac{Q_I}{P_I} = K \cdot \text{sgn}(V_i) \quad (10)$$

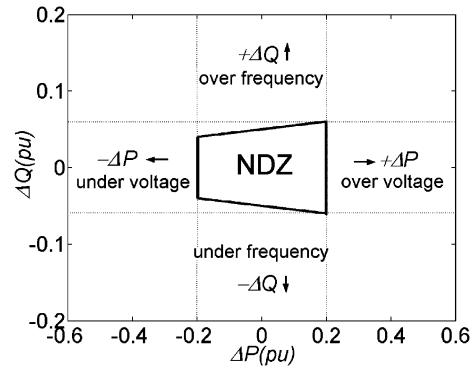


Fig. 6. Exist of nondetection zone (NDZ) of over/under voltage and frequency method.

where  $K$  denotes the reactive power perturbation and is set to 5% (or 0.05 per-unit). For this setting, a noticeable frequency deviation can be observed when the load  $q < 2.5$  (see Fig. 5). From (6), the islanding frequency for this perturbation can be calculated as

$$\omega_i = \frac{1}{\sqrt{LC}} \left( \frac{K \cdot \text{sgn}(V_i)}{2q} + 1 \right). \quad (11)$$

The frequency deviation ( $\Delta\omega_i$ ) is defined as

$$\Delta\omega_i = \omega_{i[k]} - \omega_{i[k-1]}. \quad (12)$$

When the utility is connected, it can be assumed that the DFIG is operating in parallel with a stiff voltage source. The constant real power ( $P_I$ ) or reactive power variation  $\pm 5\%$  ( $Q_I$ ) supplied by the DFIG does not have any significant effects upon the frequency or the voltage respectively at the point of interconnection. However, when the instant the utility is disconnected, a change in  $\Delta\omega_i$  is noticeable due to  $\pm 5\%$  perturbation in  $Q_I$ . When the change in  $\pm 1\% \leq \Delta\omega_i \leq \pm 2\%$  observed, the possibility of islanding is considered to be somewhat higher since it is within the specified limit of IEEE Std. 929-2000 [3], (59.3 to 60.5 Hz). This change is observed for at least for four consecutive cycles. If during this period the frequency change increases rapidly, then islanding is confirmed, and the DFIG is disconnected. However, if  $\Delta\omega_i$  continues to be within the above specified limits, the proposed algorithm reduces the DFIG real power to 80% (i.e., 0.8 per-unit) for another 10 cycles as a part of step #2. If the magnitude of the voltage  $V_i$  falls below 0.9 per-unit, the occurrence of islanding is confirmed, and the DFIG is safely disconnected. In case the magnitude of the voltage  $V_i$  is normal the DFIG is allowed to continue its operation. The proposed two step approach (described above) is robust and fast acting. Fig. 7 shows a flowchart of the proposed robust anti-islanding algorithm.

#### V. SIMULATION

In this section, simulation results are presented to illustrate the effectiveness of the proposed anti-islanding algorithm. Three possible islanding cases are simulated. The DFIG is represented by a voltage controlled current source, and its frequency is monitored every half cycle by a resettable integrator. Table I shows the parameters used in the simulation of the

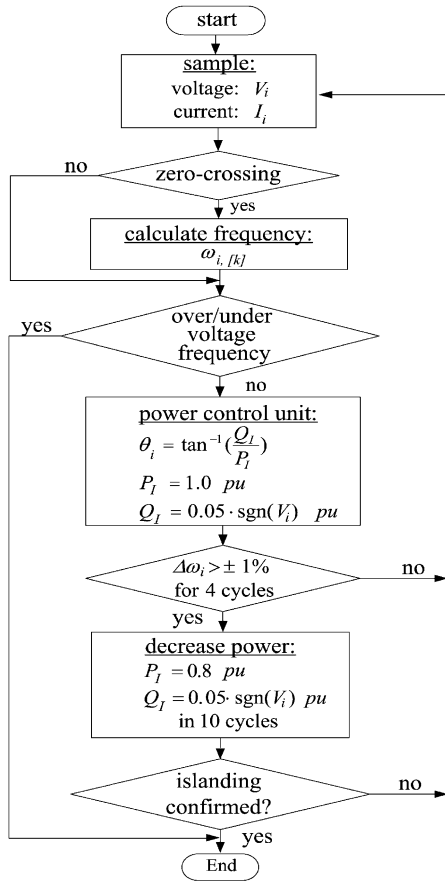


Fig. 7. Robust anti-islanding detection algorithm.

 TABLE I  
SIMULATION PARAMETERS

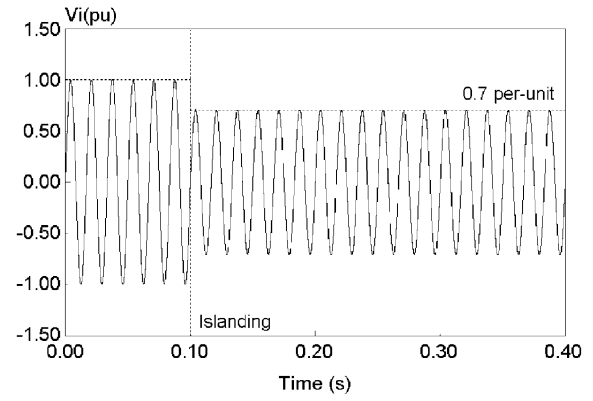
Parameters	Value
Voltage	120 V
Frequency	60 Hz
$P_{Load}$	0.5 kW, 28.80 $\Omega$
$Q_L$	1.25 kVAR, 30.56 mH
$Q_C$	1.25 kVAR, 230.25 $\mu$ F

 TABLE II  
SUMMARY OF CALCULATION, SIMULATION AND EXPERIMENTAL RESULTS

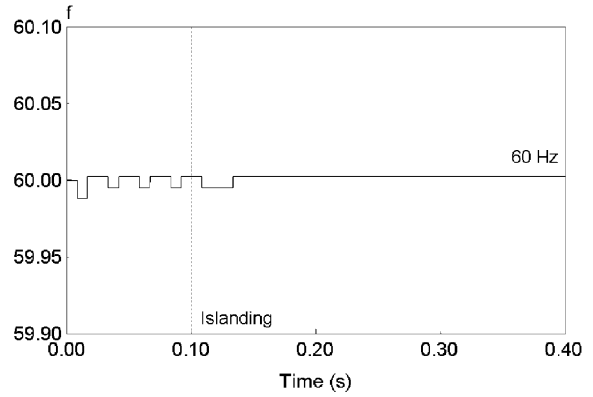
Case	$\Delta P$ (pu)	$\Delta Q$ (pu)	Calculation		Simulation		Experiment	
			$V_i$ (pu)	Hz	$V_i$ (pu)	Hz	$V_i$ (pu)	Hz
1	-0.5	0	0.71	60	0.7	60	0.7	60
2	0	0.1	1.0	61.26	1.0	61.25	1.0	61.30
3	0	0	0.89	60 $\pm$ 0.75	0.90	60 $\pm$ 0.75	0.89	60 $\pm$ 0.80

system. Real and reactive power mismatches ( $\Delta P$  and  $\Delta Q$ ) are defined in Table II and in Section II.

In Fig. 8, for case 1: real power mismatch between DFIG and the loads is large ( $\Delta P = -0.5$  per-unit and  $\Delta Q = 0$  per-unit). Under normal condition, the DFIG continuously supplies constant real power ( $P_I = 1.0$  per-unit,  $Q_I = 0$



(a)



(b)

 Fig. 8. Simulation results for case 1:  $\Delta P$  is large: (a) islanding voltage and (b) islanding frequency of  $\Delta P = -0.5$  and  $\Delta Q = 0$ .

per-unit) to the load. At instant the load disconnected, the magnitude of the voltage  $V_i$  immediately drops to 0.70 per-unit [Fig. 8(a)] due to insufficient real power supplied from the DFIG [see (8)]. The occurrence of islanding can be easily detected by monitoring the under voltage. It is noted that the frequency does not alter significantly since  $\Delta Q$  is zero.

Fig. 9 shows the simulation results for case 2: for  $\Delta P = 0$  and  $\Delta Q = 0.1$  per-unit. In this case, the DFIG real power  $P_I$  is same as the load  $P_{Load}$ ; however, the DFIG reactive power  $Q_I$  exceeds  $Q_{Load}$  by 0.1 per-unit. At the instant the utility is disconnected, it is seen that the magnitude of  $V_i$  is unaltered, but the frequency increases to 61.25 Hz. This new operating frequency results from a larger reactive power mismatch [see (6)]. Since this exceeds the IEEE Std. 929-2000 [3] specified limit (59.3 to 60.5 Hz), islanding condition is positively confirmed.

Fig. 10 shows the simulation results for case 3: both the real and reactive power mismatches are small ( $\Delta P \approx 0$  per-unit and  $\Delta Q \approx 0$ ). For this condition to exist, the DFIG real and reactive power must match the connected load. That is  $P_I \approx P_{Load}$  and  $Q_I \approx Q_{Load}$ . From the previous analysis, it is clear that this is the most difficult scenario to detect islanding. The proposed robust anti-islanding algorithm is employed. In this case, the DFIG real power is maintained constant, and its reactive power is perturbed by  $\pm 5\%$ . At the instant the utility disconnected, from Fig. 10(b), it is noted that a frequency deviation is observed ( $\Delta\omega_i = \pm 0.50$  Hz). According to the proposed algorithm, the DFIG is allowed to continue its operation

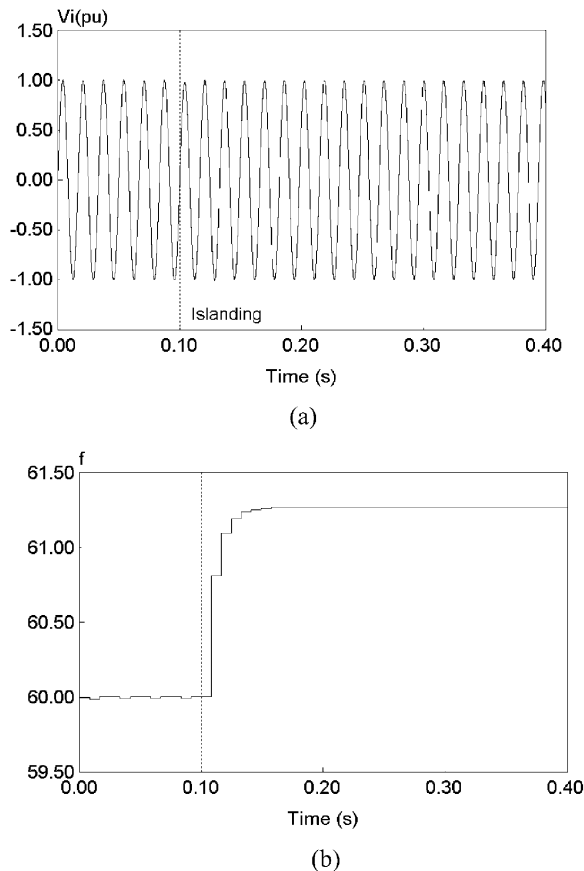


Fig. 9. Simulation results for case 2:  $\Delta P$  is small and  $\Delta Q$  is large: (a) islanding voltage and (b) islanding frequency of  $\Delta P = 0$  and  $\Delta Q = 0.1$ .

as long as frequency variation is within the specified limit (59.3 to 60.5 Hz). In the mean time, the algorithm recognizes the frequency variation for over four consecutive cycles, and the DFIG real power  $P_r$  is then reduced to 80% level for the next ten cycles. It is noted in Fig. 10(a) the terminal voltage magnitude ( $V_i$ ) is reduced to 0.9 per-unit, thus positively confirming islanding.

## VI. EXPERIMENTAL RESULTS

Fig. 11 shows the experimental setup of a single phase fuel cell inverter rated at 0.5 kW, 120 V, 60 Hz connected to the utility. The inverter is controlled in current control mode employing a TMS-320-F243 digital signal processor (DSP). The proposed robust anti-islanding algorithm is implemented in DSP via software. Under normal condition, the inverter (DFPG) is programmed to continuously supply the available fuel cell power to the utility. The reactive power of the inverter is constantly perturbed by  $\pm 5\%$  as described in Sections II–V. Both real and reactive power supplied by the DFIG can be controlled by altering the phase shift between utility voltage and inverter current.

Fig. 12 shows the normal operation of the DFIG when connected to the utility. Fig. 13 shows significant terminal voltage drop to 0.70/unit due to large real power mismatch ( $\Delta P = -0.50$  per – unit) which described in islanding case 1. It is noticed that inverter current is increased after reduction of terminal voltage to maintain constant output power. Fig. 14 shows

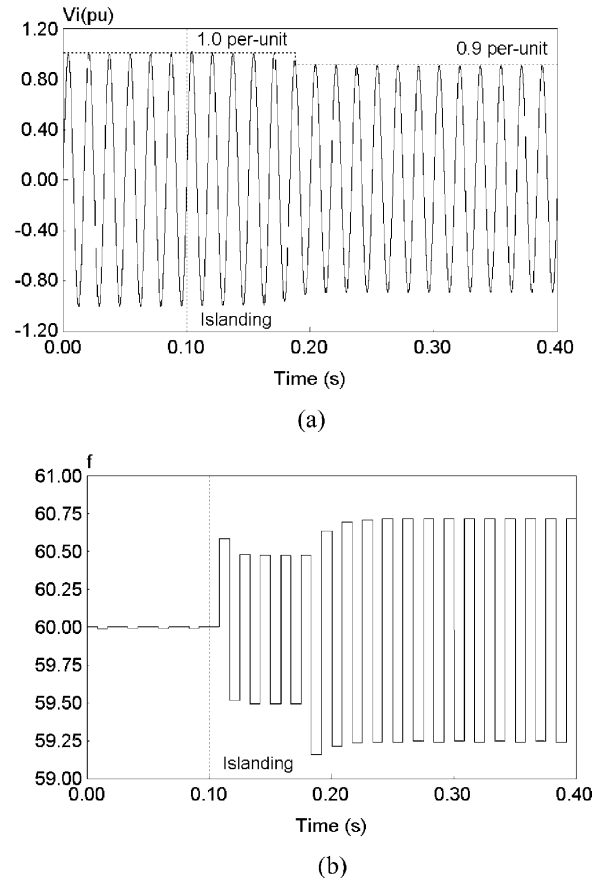


Fig. 10. Simulation results for case 3:  $\Delta P$  and  $\Delta Q$  is small and a robust anti-islanding algorithm is applied (a) islanding voltage and (b) islanding frequency of  $\Delta P \approx 0$  and  $\Delta Q \approx 0$ .

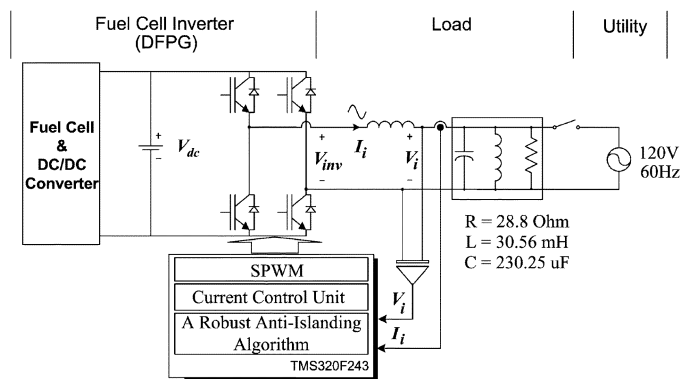


Fig. 11. Experimental setup.

noticeable frequency change when islanding case 2 occurs. Frequency is increased to 61.3 Hz due to reactive power mismatch ( $\Delta Q = 0.1$ ), but terminal voltage remains the same as nominal utility voltage because of zero real power mismatch. Fig. 15 shows the noticeable frequency deviation ( $\omega_i = \pm 0.60$  Hz) when islanding occurs for case 3. The inverter (DFPG) continues to operate (Fig. 15) for four cycles and initiates the real power reduction to 0.8 per-unit, upon which the voltage ( $V_i$ ) is shown to reduce confirming islanding. Experimental results of all three cases are compared to simulation results and analytical equations (Section II) in Table II.

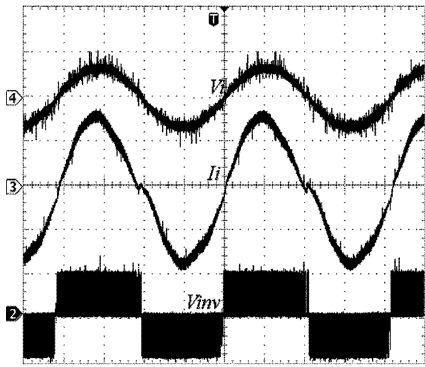


Fig. 12. Experimental result of normal operation of the DFGP connected to the utility, CH2: fuel cell inverter voltage ( $V_{inv}$ ) 250 V/div, CH3: fuel cell inverter current ( $I_i$ ) 4 A/div, CH4 terminal voltage (utility voltage,  $V_t$ ), 250 V/div.

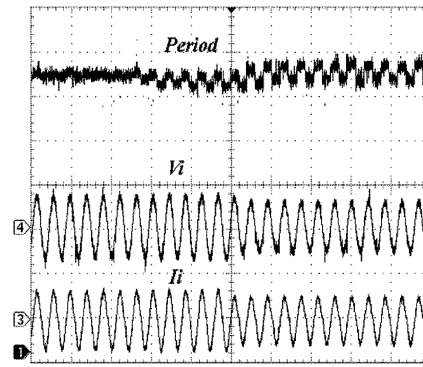


Fig. 15. Experimental result of islanding detection by the developed robust anti-islanding algorithm, CH1: period of terminal voltage 2.60 ms/div, CH3: fuel cell inverter current ( $I_i$ ) 10 A/div CH4: terminal voltage (islanding, voltage,  $V_t$ ), 250 V/div.

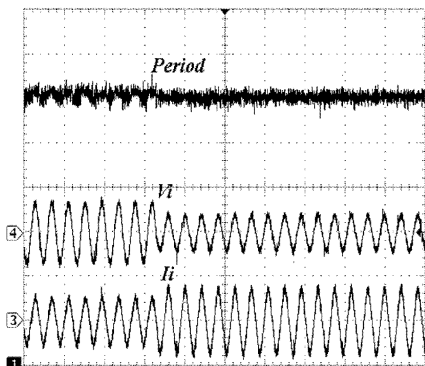


Fig. 13. Experimental result of islanding case 1, CH1: period of terminal voltage 2.60 ms/div, CH3: fuel cell inverter current ( $I_i$ ) 10 A/div CH4: terminal voltage (islanding, voltage,  $V_t$ ), 250 V/div.

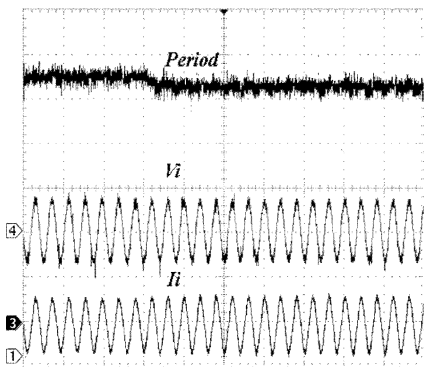


Fig. 14. Experimental result of islanding case 2, CH1: period of terminal voltage 2.60 ms/div, CH3: fuel cell inverter current ( $I_i$ ) 10 A/div CH4: terminal voltage (islanding, voltage,  $V_t$ ), 250 V/div.

VII. LIMITATION

The proposed power control algorithm discussed has been shown to be a viable technique. However, if multiple DFGPs of smaller power ratings are connected to the utility, and each of them operates independently, then the proposed power control algorithm may fail and/or malfunction [14]. To overcome this barrier, a cross correlation index of a rate of change of frequency with respect to reactive power variation can be introduced and islanding can be detected. Even though the change in

frequency deviation is relatively small ( $\Delta\omega_i \leq \pm 1\%$ ), if the frequency deviation  $\Delta\omega_i$  strongly depends on the output reactive power variation  $\pm 5\%$  (i.e., a cross correlation index  $> 80\%$ ), the occurrence of islanding can be confirmed. This correlation approach is shown to be more accurate and applicable in multiple DFGP's connected to utility.

VIII. CONCLUSION

In this paper, a robust anti-islanding algorithm for utility interconnection of distributed fuel cell power generation (DFGP) has been presented. It has been shown via analysis that the islanding voltage depends on real power mismatch alone, and the islanding frequency is a function of both real and reactive power. Following to analysis, the robust anti-islanding algorithm has been fully analyzed and developed. This detection method has been shown to be robust and fast acting (operable in one cycle), and it significantly reduces the nondetection zone. Simulation and experimental results confirm the effectiveness of the proposed method.

REFERENCES

- [1] P. Enjeti, "Chapter 8: Power conditioning systems for fuel cell systems," in *Fuel Cell Handbook*, Sixth ed. Washington, DC: U.S. Dept. of Energy, 2002.
- [2] J. Stevens, R. Bonn, J. Ginn, S. Gonzalez, and G. Kern, "Development and testing of an approach to anti-islanding in utility-interconnected photovoltaic systems," Tech. Rep. SAND 2000-1939, Sandia Nat. Labs, Albuquerque, NM, 2000.
- [3] *IEEE Recommended Practice for Utility Interface of Photovoltaic (PV) Systems*, IEEE Std. 929-2000, 2000.
- [4] *Standard for Interconnecting Distributed Resources With Electric Power Systems*, IEEE Std. 1547-2003.
- [5] H. Kobayashi, K. Takigawa, and E. Hashimoto, "Method for preventing phenomenon of utility grid with a number of small scale PV systems," in *Proc. 22nd IEEE Photovoltaic Specialists Conf.*, 1991, pp. 695-700.
- [6] A. Kitamura, M. Okamoto, F. Yamamoto, K. Nakaji, H. Matsuda, and K. Hotta, "Islanding phenomenon elimination study at Rokko test center," in *Proc. 1st IEEE World Conf. Photovoltaic Energy Conversion*, 1994, pp. 759-762.
- [7] G. A. Kern, "Sunsine300 utility interactive AC module anti-islanding test results," in *Proc. 26th IEEE Photovoltaic Systems Conf.*, 1997, pp. 1265-1268.
- [8] G. A. Smith, P. A. Onions, and D. G. Infield, "Predicting islanding operation of grid connected PV inverters," *Proc. Inst. Elect. Eng.*, vol. 147, no. 1, pp. 1-6, Jan. 2000.
- [9] M. E. Ropp, M. Begovic, and A. Rohatgi, "Analysis and performance assessment of the active frequency drift method of islanding prevention," *IEEE Trans. Energy Conv.*, vol. 14, pp. 810-816, Sept. 1999.

- [10] S. Yuyama, T. Ichinose, K. Kimoto, T. Itami, T. Ambo, C. Okado, K. Nakajima, S. Hojo, H. Shinohara, S. Ioka, and M. Kuniyoshi, "A high speed frequency shift method as a protection for islanding phenomena of utility interactive PV systems," *Sol. Energy Mater. Sol. Cells*, vol. 35, no. 1–4, pp. 477–486, 1994.
- [11] M. E. Ropp, "Design issues for grid-connected photovoltaic systems," Ph.D. dissertation, Georgia Inst. Technol., Atlanta, 1998.
- [12] G. Hung, C. Chang, and C. Chen, "Automatic phase-shift method for islanding detection of grid-connected photovoltaic inverters," *IEEE Trans. Energy Conv.*, vol. 18, pp. 169–173, Mar. 2003.
- [13] V. Task, "Evaluation of islanding detection methods for photovoltaic utility-interactive power systems," Tech. Rep. IEA-PVPS T5-09:2002, 2002.
- [14] C. Jeraputra, P. N. Enjeti, and I. H. Hwang, "Development of a robust anti-islanding algorithm for utility interconnection of distributed fuel cell powered generation," in *Proc. APEC'04 Conf.*, vol. 3, 2004, pp. 1534–1540.



**Chutthaval Jeraputra** received B.E. degree in electrical engineering from King Mongkut's Institute of Technology (Ladkrabang), Thailand, in 1994 and is currently pursuing the Ph.D. degree in the Electrical Engineering Department, Texas A&M University, College Station.

His research interests are primarily in advanced power electronic converters and their control and utility interconnection issues of distributed generations.



**Prasad N. Enjeti** (M'85–SM'88–F'00) received the B.E. degree from Osmania University, Hyderabad, India, in 1980, the M.Tech. degree from the Indian Institute of Technology, Kanpur, in 1982, and the Ph.D. degree from Concordia University, Montreal, QC, Canada, in 1988, all in electrical engineering.

In 1988, he became an Assistant Professor in the Department of Electrical Engineering, Texas A&M University (TAMU), College Station. In 1994, he was promoted to Associate Professor and in 1998 he became a Full Professor. His primary research interests

are advance converters for power supplies and motor drives, power quality issues and active power filter development, converters for fuel cell microturbine, wind energy systems, and power electronic hardware for flywheel and ultracapacitor type energy storage/discharge devices for ride-through and utility interface issues. He holds four U.S. patents and has licensed two new technologies to the industry so far. He is the Lead Developer of the Power Electronics/Power Quality and Fuel Cell Power Conditioning Laboratories, TAMU, and is actively involved in many projects with industries while engaged in teaching, research, and consulting in the area of power electronics, motor drives, power quality, and clean power utility interface issues.

Dr. Enjeti received the IEEE-IAS Second and Third best paper awards in 1993, 1996, 1998, 1999, and 2001, respectively, the second best IEEE-IA Transaction Paper Award, 1994–1995, the IEEE-IAS Magazine Prize Article Award in 1996, the Class of 2001 TAMU Faculty Fellow Award, and the 2001 future energy challenge award, grand prize, from the Department of Energy (DoE). He is a Registered Professional Engineer in the state of Texas.